

# Laplace-transformed atomic orbital-based Møller–Plesset perturbation theory for relativistic two-component Hamiltonians

Benjamin Helmich-Paris,<sup>1, a)</sup> Michal Repisky,<sup>2, b)</sup> and Lucas Visscher<sup>1, c)</sup>

<sup>1)</sup>*Section of Theoretical Chemistry, VU University Amsterdam, De Boelelaan 1083, 1081 HV Amsterdam, The Netherlands*

<sup>2)</sup>*CTCC, Department of Chemistry, UiT The Arctic University of Norway, N-9037 Tromø Norway*

(Dated: 25 March 2022)

We present a formulation of Laplace-transformed atomic orbital-based second-order Møller–Plesset perturbation theory (MP2) energies for two-component Hamiltonians in the Kramers-restricted formalism. This low-order scaling technique can be used to enable correlated relativistic calculations for large molecular systems. We show that the working equations to compute the relativistic MP2 energy differ by merely a change of algebra (quaternion instead of real) from their non-relativistic counterparts. With a proof-of-principle implementation we study the effect of the nuclear charge on the magnitude of half-transformed integrals and show that for light elements spin-free and spin-orbit MP2 energies are almost identical. Furthermore, we investigate the effect of separation of charge distributions on the Coulomb and exchange energy contributions, which show the same long-range decay with the inter-electronic / atomic distance as for non-relativistic MP2. A linearly scaling implementation is possible if the proper distance behavior is introduced to the quaternion Schwarz-type estimates as for non-relativistic MP2.

## I. INTRODUCTION

The most accurate way amongst today’s standard approaches to account for relativistic effects in molecules is to solve the Dirac equation for the large (LC) and small two-component (SC) part of the wave function.<sup>1</sup> Employing the full four-component (4C) methodology of the Dirac equation yields solutions for both positronic and electronic states. An accurate approximation to the Dirac equation that gives electronic — positive energy — solutions only is the exact (X) two-component (2C) method,<sup>2</sup> in which the Dirac Hamiltonian is reduced to a 2 x 2 matrix form. While exact for a given one-body operator, the X2C method usually includes the approximation of omitting the picture-change transformation of two-electron integrals. Especially for correlated calculations, this makes the algorithm very efficient as molecular integrals then require evaluation of only LC atomic-orbital (AO) two-electron integrals. Since the SC AO basis can be up to 3 times larger than the LC AO basis, if the unrestricted kinetic balance condition is employed, the overhead of the integral calculation and transformation is then reduced immensely.<sup>3</sup>

With a relativistic 2C Hamiltonian the overhead of the Dirac equation is thus reduced, but accurate wave function methods still feature a steep scaling of the computational work with the system size  $N$ , e.g. second-order Møller–Plesset perturbation theory<sup>4</sup> (MP2) scales with  $\mathcal{O}(N^5)$ . To overcome this computational bottleneck, several reduced scaling approaches were proposed for MP2 over the years.<sup>5–9</sup> One of the most successful approaches originates from Almlöf<sup>5,10</sup> and Häser<sup>6</sup> where the MP2 correlation energy is formulated purely in the AO basis by means of a numerical Laplace transformation (LT) of orbital-energy denominators. By employing estimates for integral screening, low-order scaling implementations were proposed by Häser<sup>6</sup> and Ayala and Scuseria.<sup>7</sup> Ochsenfeld and his co-workers showed how to achieve linear scaling of all computationally demanding steps by accounting for the distance-dependent decay of integrals,<sup>8,11,12</sup> and their implementation currently allows for calculations on molecules with 1000 atoms and more on a single core.<sup>12</sup> The same authors have also presented a promising computational performance for large AO basis sets that include high angular momentum and / or diffuse basis functions when the LT AO-based approach is combined with Cholesky decomposition of two-electron integrals.<sup>9</sup> Alternatively, the performance of the LT AO-based approach when large basis sets are employed can also be remedied with a modern formulation of explicitly correlated MP2-F12<sup>13,14</sup> in the AO

basis, which became available recently.<sup>15</sup>

In the current work, we present for the first time formulae for LT AO-based MP2 correlation energy for relativistic 2C Hamiltonians in a Kramers-restricted (KR) formalism. The additional spin orbit (SO)-induced complexity of the formulae is discussed by comparing with non-relativistic (NR) LT AO-MP2 and conventional KR spinor-based approaches. Furthermore, we present an adaptation of the Schwarz-type estimates, which are employed to screen shell quadruple contributions to the MP2 correlation energy, to the 2C formalism. Those Schwarz-type estimates<sup>6</sup> pave the way to develop a linearly scaling 2C LT AO-MP2 implementation once they are combined with the proper distance-dependence terms.<sup>12</sup> With a proof-of-principle implementation we analyze the effect of the nuclear charge and the separation of electronic charge distributions on the correlation energy contributions.

## II. THEORY

### A. MP2 energy for 1C, 2C, and 4C Hamiltonians

The MP2 correlation energy is given by

$$E_{\text{MP2}} = -\frac{1}{4} \sum_{IJAB} \frac{1}{\Delta_{AIBJ}} |(IA||JB)|^2 \quad (1)$$

$$= -\frac{1}{2} \sum_{IJAB} \frac{1}{\Delta_{AIBJ}} ((BJ|AI) - (AJ|BI)) (IA|JB) \quad (2)$$

$$= E_J - E_K. \quad (3)$$

In Eq. (1),  $(IA||JB)$  are anti-symmetrized two-electron integrals  $(IA|JB)$  that involve active occupied ( $I, J$ ) and active virtual ( $A, B$ ) spinors;  $\Delta_{AIBJ}$  is the denominator

$$\Delta_{AIBJ} = \varepsilon_A - \varepsilon_I + \varepsilon_B - \varepsilon_J \quad (4)$$

that comprises real orbital energies  $\varepsilon_P$  with  $P = I, A, J,$  and  $B$ . Note that Eq. (1) is valid for both NR and relativistic Hamiltonians when spin orbitals and 4C (or 2C) spinors are employed, respectively. This equation furthermore only assumes a single determinant reference wave function and is therefore applicable to both restricted and unrestricted Hartree–Fock wave functions. In practice, one usually deals with closed-shell systems and it is therefore efficient to make use of Kramers symmetry<sup>16</sup> in the Hartree–Fock self-consistent field procedure. Spinor energies are then doubly degenerate and the number of unique variational

parameters is reduced by a factor of two as the expansion coefficients for pairs of spinors are related. We will assume such a restricted optimization and label two spinors that form a Kramers pair by the lowercase symbols  $p$  and  $\tilde{p}$ . These spinors can be expressed in a set of real AO basis functions  $\chi_\mu$  as

$$\phi_p = \begin{pmatrix} \phi_p^\alpha \\ \phi_p^\beta \end{pmatrix} = \begin{pmatrix} \sum_\mu \chi_\mu C_{\mu p}^\alpha \\ \sum_\mu \chi_\mu C_{\mu p}^\beta \end{pmatrix} \quad \phi_{\tilde{p}} = \begin{pmatrix} \phi_{\tilde{p}}^\alpha \\ \phi_{\tilde{p}}^\beta \end{pmatrix} = \begin{pmatrix} \sum_\mu \chi_\mu (-C_{\mu p}^{\beta*}) \\ \sum_\mu \chi_\mu (C_{\mu p}^{\alpha*}) \end{pmatrix}; \quad (5)$$

a form which clearly displays the Kramers relation between the coefficients. This expansion is valid for NR, scalar-relativistic (SR), and SO relativistic spinor optimization and can be defined to encompass both 2C and 4C spinors. In the latter case, the basis set is divided into separate sets of LC and SC expansion functions and coefficients, which describe respectively the upper and lower components of the 4C spinor.

In the X2C approximation, that we focus on in the current work, the Dirac–Coulomb Hamiltonian is reduced to an effective 2C form and picture change corrections on the two-electron operator are neglected. With these approximations AO integrals reduce to their familiar NR form

$$(\kappa\lambda|\mu\nu) = \int \int \chi_\kappa(\mathbf{r}_1)\chi_\lambda(\mathbf{r}_1)\frac{1}{r_{12}}\chi_\mu(\mathbf{r}_2)\chi_\nu(\mathbf{r}_2)d\mathbf{r}_1d\mathbf{r}_2 \quad (6)$$

and can be evaluated using standard techniques.

Relativity is manifest only in the MO coefficients, with scalar relativistic effects merely changing their value but not changing the structure of the coefficient matrices. NR and SR approaches have real, block diagonal, coefficient matrices  $\mathbf{C}_p^\alpha = \mathbf{C}_{\tilde{p}}^\beta$ ;  $\mathbf{C}_p^\beta = \mathbf{C}_{\tilde{p}}^\alpha = \mathbf{0}$ , while SO approaches yield complex matrices for which  $\mathbf{C}_p^\beta \neq 0$ . It is the latter effect which makes relativistic correlated calculation more expensive than their NR counterparts.

## B. LT AO-based MP2 for 1C Hamiltonians

By means of the (numerical) LT, it has been shown initially by Almlöf and Häser<sup>5,6,10</sup> that an expansion of the orbital-energy denominator (Eq. (4)) according to

$$\frac{1}{\Delta_{aibj}} = \int_0^\infty \exp(-\Delta_{aibj} t) dt \approx \sum_{z=1}^{n_z} \omega_z \exp(-\Delta_{aibj} t_z) \quad (7)$$

results in a formulation for the Coulomb ( $J$ ) and exchange contribution ( $K$ ),<sup>6,7,11,17</sup>

$$E_{\text{MP2}} = \sum_{z=1}^{n_z} e_J^{(z)} - e_K^{(z)}, \quad (8)$$

solely in terms of intermediates in the AO basis. In Eqs. (7) – (8)  $n_z$  denotes a pre-defined number of quadrature points represented by  $\{\omega_z, t_z\}$ . For the NR Hamiltonian and restricted HF reference wave functions, occupied

$$\begin{aligned} \underline{\mathbf{P}}^{(z)} &= |\omega_z|^{1/4} \mathbf{C}^o \exp(+\boldsymbol{\varepsilon}^o t_z) (\mathbf{C}^o)^T \\ &= |\omega_z|^{1/4} \exp(+t_z \mathbf{P} \mathbf{F}) \mathbf{P} \end{aligned} \quad (9)$$

and virtual pseudo-density matrices

$$\begin{aligned} \bar{\mathbf{P}}^{(z)} &= |\omega_z|^{1/4} \mathbf{C}^v \exp(-\boldsymbol{\varepsilon}^v t_z) (\mathbf{C}^v)^T \\ &= |\omega_z|^{1/4} \exp(-t_z \mathbf{Q} \mathbf{F}) \mathbf{Q} \end{aligned} \quad (10)$$

are used to transform the two-electron integrals to write the  $J$  and  $K$  contributions

$$e_J^{(z)} = 2 \sum_{\mu\nu\kappa\lambda} (\underline{\mu}\bar{\nu}|\kappa\lambda)^{(z)} (\mu\nu|\underline{\kappa}\bar{\lambda})^{(z)}, \quad (11)$$

$$e_K^{(z)} = \sum_{\mu\nu\kappa\lambda} (\underline{\mu}\bar{\nu}|\kappa\lambda)^{(z)} (\mu\bar{\lambda}|\underline{\kappa}\nu)^{(z)} \quad (12)$$

in terms of half-transformed integrals (HTI)

$$(\underline{\mu}\bar{\nu}|\kappa\lambda)^{(z)} = \sum_{\mu'} \underline{P}_{\mu'\mu}^{(z)} \left( \sum_{\nu'} \bar{P}_{\nu\nu'}^{(z)} (\mu'\nu'|\kappa\lambda) \right), \quad (13)$$

$$(\mu\bar{\lambda}|\underline{\kappa}\nu)^{(z)} = \sum_{\kappa'} \underline{P}_{\kappa'\kappa}^{(z)} \left( \sum_{\lambda'} \bar{P}_{\lambda\lambda'}^{(z)} (\mu\lambda'|\kappa'\nu) \right). \quad (14)$$

In Eqs. (9) – (10),  $\mathbf{F}$  is the Fock matrix and  $\boldsymbol{\varepsilon}$  the orbital-energy vector;  $o$  and  $v$  indicate the set of all active occupied and virtual orbitals, respectively. In Eqs. (13) – (14) and in the following  $\mu$ ,  $\nu$ ,  $\kappa$ , and  $\lambda$  denote scalar AO basis functions. Since the two density matrices  $\mathbf{P}$  and  $\mathbf{Q}$  are related through the constant AO overlap matrix  $\mathbf{S}$  by

$$\mathbf{P} = \mathbf{C}^o (\mathbf{C}^o)^T, \quad (15)$$

$$\mathbf{P} + \mathbf{Q} = \mathbf{S}^{-1}, \quad (16)$$

the NR MP2 energy in Eq. (8) is a functional of the HF density matrix  $\mathbf{P}$ .<sup>17</sup> To simplify the formulae, the index  $z$  that denotes the quadrature point is omitted in the following when appropriate.

### C. LT AO-based MP2 for 2C Hamiltonians

We can repeat this procedure for relativistic spinors in which we use the Kramers' symmetry of the MO coefficients to reduce the number of operations. If spinors are generated in a KR algorithm, the full spinor set is subdivided in two sets of spinors with related coefficients (Eq. (5)). This then leads to the classification of 16 different sub-blocks of two-electron integrals ( $IA|JB$ ):

$$\begin{aligned}
& (ia|jb) (\tilde{i}\tilde{a}|jb) (\tilde{i}a|\tilde{j}b) (\tilde{i}a|\tilde{j}b) \\
& (ia|\tilde{j}b) (ia|\tilde{j}b) (i\tilde{a}|jb) (\tilde{i}a|jb) \\
& (\tilde{i}\tilde{a}|\tilde{j}b) (ia|\tilde{j}b) (i\tilde{a}|\tilde{j}b) (i\tilde{a}|\tilde{j}b) \\
& (\tilde{i}\tilde{a}|\tilde{j}b) (\tilde{i}\tilde{a}|\tilde{j}b) (\tilde{i}a|\tilde{j}b) (\tilde{i}a|\tilde{j}b),
\end{aligned} \tag{17}$$

for which it is easy to show that the last 8 integral blocks are the complex conjugate of the first 8. Furthermore, the integrals on the second and the fourth line are zero if the system under consideration has (at least) a two-fold element of symmetry (mirror plane or rotation axis). The Coulomb energy

$$\begin{aligned}
E_J &= \frac{1}{2} \sum_{JIBA} \frac{1}{\Delta_{AIBJ}} (BJ|AI)(IA|JB) \\
&= \sum_{jiba} \frac{1}{\Delta_{aibj}} \left( (ai|bj)(ia|jb) + (\tilde{a}\tilde{i}|bj)(\tilde{i}\tilde{a}|jb) \right. \\
&\quad \left. + 2(a\tilde{i}|bj)(\tilde{i}a|jb) + 2(\tilde{a}i|bj)(i\tilde{a}|jb) \right. \\
&\quad \left. + (a\tilde{i}|b\tilde{j})(\tilde{i}a|\tilde{j}b) + (a\tilde{i}|\tilde{b}j)(\tilde{i}a|j\tilde{b}) \right)
\end{aligned} \tag{18}$$

comprises 6 contributions that are real even without exploiting Kramers symmetry because one of the integrals in each of the products in Eq. (18) is the complex conjugate of the one it is multiplied with. In the KR formalism, the exchange energy

$$\begin{aligned}
E_K &= \sum_{jiba} \frac{1}{\Delta_{aibj}} \left( \text{Re}((bi|aj)(ia|jb)) + \text{Re}((b\tilde{i}|\tilde{a}j)(\tilde{i}\tilde{a}|jb)) \right. \\
&\quad \left. + 2\text{Re}((b\tilde{i}|aj)(\tilde{i}a|jb)) + 2\text{Re}((bi|\tilde{a}j)(i\tilde{a}|jb)) \right. \\
&\quad \left. + \text{Re}((b\tilde{i}|a\tilde{j})(\tilde{i}a|\tilde{j}b)) + \text{Re}((b\tilde{i}|\tilde{a}j)(\tilde{i}a|j\tilde{b})) \right)
\end{aligned} \tag{20}$$

comprises 6 real contributions as the integral products in (20) appear in complex conjugate pairs with imaginary parts canceling each other. The spinor-based integral products in Eqs. (18) and (20) can be factorized in terms of two-electron integrals and density matrices as for the NR case. Here, we only show the working equations in their most condensed formulation of 2C AO-based MP2. For a complete derivation we refer to the supporting information.<sup>18</sup>

Before proceeding, we introduce quaternion algebra<sup>19</sup> for the KR formalism as it is the most compact notation and results in working equations that feature the least number of computational operations. The quaternion spinor coefficients are given by

$$\begin{aligned}
{}^q\mathbf{C} &= \mathbf{C}^\alpha - (\mathbf{C}^\beta)^* j \\
&= \text{Re}(\mathbf{C}^\alpha) + \text{Im}(\mathbf{C}^\alpha) i - \text{Re}(\mathbf{C}^\beta) j + \text{Im}(\mathbf{C}^\beta) k \\
&= \mathbf{C}^0 + \mathbf{C}^1 i + \mathbf{C}^2 j + \mathbf{C}^3 k
\end{aligned} \tag{21}$$

and from Eq. (21) the quaternion density matrices  ${}^q\mathbf{P}$  and  ${}^q\mathbf{Q}$  can be constructed by

$${}^q\mathbf{P} = {}^q\mathbf{C}^o ({}^q\mathbf{C}^o)^\dagger = \mathbf{P}^0 + \mathbf{P}^1 i + \mathbf{P}^2 j + \mathbf{P}^3 k, \tag{22}$$

$${}^q\mathbf{P} + {}^q\mathbf{Q} = \mathbf{S}^{-1}, \tag{23}$$

where  $\mathbf{P}^0, \mathbf{Q}^0$  and  $\mathbf{P}^{q_1}, \mathbf{Q}^{q_1}$  with  $q_1 = 1, \dots, 3$  are real symmetric and anti-symmetric matrices, respectively.

As for the NR Hamiltonian,<sup>17</sup> the MP2 energy is a functional of the quaternion HF density matrix  ${}^q\mathbf{P}$ , which facilitates a formulation and implementation without spinors purely in the AO basis. For relativistic 2C Hamiltonians, the Coulomb-

$$\begin{aligned}
e_J^{(z)} &= 2 \sum_{\mu\nu\kappa\lambda} \sum_{\mu'\nu'\kappa'\lambda'} \left( \underline{P}_{\mu'\mu}^0 \bar{P}_{\nu\nu'}^0 - \underline{P}_{\mu'\mu}^1 \bar{P}_{\nu\nu'}^1 - \underline{P}_{\mu'\mu}^2 \bar{P}_{\nu\nu'}^2 - \underline{P}_{\mu'\mu}^3 \bar{P}_{\nu\nu'}^3 \right) \\
&\quad \left( \underline{P}_{\kappa'\kappa}^0 \bar{P}_{\lambda\lambda'}^0 - \underline{P}_{\kappa'\kappa}^1 \bar{P}_{\lambda\lambda'}^1 - \underline{P}_{\kappa'\kappa}^2 \bar{P}_{\lambda\lambda'}^2 - \underline{P}_{\kappa'\kappa}^3 \bar{P}_{\lambda\lambda'}^3 \right) \\
&\quad (\mu'\nu'|\kappa'\lambda')(\mu\nu|\kappa\lambda)
\end{aligned} \tag{24}$$

$$= 2 \sum_{\mu\nu\kappa\lambda} \sum_{\mu'\nu'\kappa'\lambda'} \left( \text{Re}({}^q\underline{\mathbf{P}}_{\mu'\mu} \quad {}^q\bar{\mathbf{P}}_{\nu\nu'}) \text{Re}({}^q\underline{\mathbf{P}}_{\kappa'\kappa} \quad {}^q\bar{\mathbf{P}}_{\lambda\lambda'}) \right) (\mu'\nu'|\kappa'\lambda')(\mu\nu|\kappa\lambda) \tag{25}$$

$$= 2 \sum_{\mu\nu\kappa\lambda} \text{Re}(({}^q\underline{\boldsymbol{\mu}} \quad {}^q\bar{\boldsymbol{\nu}}|\kappa\lambda)) \text{Re}((\mu\nu|{}^q\underline{\boldsymbol{\kappa}} \quad {}^q\bar{\boldsymbol{\lambda}})) \tag{26}$$

and exchange contributions

$$\begin{aligned}
e_K^{(z)} = & \sum_{\mu\nu\kappa\lambda} \sum_{\mu'\nu'\kappa'\lambda'} \left[ \left( \underline{P}_{\mu'\mu}^0 \bar{P}_{\lambda\nu'}^0 - \underline{P}_{\mu'\mu}^1 \bar{P}_{\lambda\nu'}^1 - \underline{P}_{\mu'\mu}^2 \bar{P}_{\lambda\nu'}^2 - \underline{P}_{\mu'\mu}^3 \bar{P}_{\lambda\nu'}^3 \right) \right. \\
& \left( \underline{P}_{\kappa'\kappa}^0 \bar{P}_{\nu\lambda'}^0 - \underline{P}_{\kappa'\kappa}^1 \bar{P}_{\nu\lambda'}^1 - \underline{P}_{\kappa'\kappa}^2 \bar{P}_{\nu\lambda'}^2 - \underline{P}_{\kappa'\kappa}^3 \bar{P}_{\nu\lambda'}^3 \right) \\
& - \left( \underline{P}_{\mu'\mu}^0 \bar{P}_{\lambda\nu'}^1 + \underline{P}_{\mu'\mu}^1 \bar{P}_{\lambda\nu'}^0 - \underline{P}_{\mu'\mu}^2 \bar{P}_{\lambda\nu'}^3 + \underline{P}_{\mu'\mu}^3 \bar{P}_{\lambda\nu'}^2 \right) \\
& \left( \underline{P}_{\kappa'\kappa}^0 \bar{P}_{\nu\lambda'}^1 + \underline{P}_{\kappa'\kappa}^1 \bar{P}_{\nu\lambda'}^0 - \underline{P}_{\kappa'\kappa}^2 \bar{P}_{\nu\lambda'}^3 + \underline{P}_{\kappa'\kappa}^3 \bar{P}_{\nu\lambda'}^2 \right) \\
& - \left( \underline{P}_{\mu'\mu}^0 \bar{P}_{\lambda\nu'}^2 + \underline{P}_{\mu'\mu}^1 \bar{P}_{\lambda\nu'}^3 + \underline{P}_{\mu'\mu}^2 \bar{P}_{\lambda\nu'}^0 - \underline{P}_{\mu'\mu}^3 \bar{P}_{\lambda\nu'}^1 \right) \\
& \left( \underline{P}_{\kappa'\kappa}^0 \bar{P}_{\nu\lambda'}^2 + \underline{P}_{\kappa'\kappa}^1 \bar{P}_{\nu\lambda'}^3 + \underline{P}_{\kappa'\kappa}^2 \bar{P}_{\nu\lambda'}^0 - \underline{P}_{\kappa'\kappa}^3 \bar{P}_{\nu\lambda'}^1 \right) \\
& - \left( \underline{P}_{\mu'\mu}^0 \bar{P}_{\lambda\nu'}^3 - \underline{P}_{\mu'\mu}^1 \bar{P}_{\lambda\nu'}^2 + \underline{P}_{\mu'\mu}^2 \bar{P}_{\lambda\nu'}^1 + \underline{P}_{\mu'\mu}^3 \bar{P}_{\lambda\nu'}^0 \right) \\
& \left. \left( \underline{P}_{\kappa'\kappa}^0 \bar{P}_{\nu\lambda'}^3 - \underline{P}_{\kappa'\kappa}^1 \bar{P}_{\nu\lambda'}^2 + \underline{P}_{\kappa'\kappa}^2 \bar{P}_{\nu\lambda'}^1 + \underline{P}_{\kappa'\kappa}^3 \bar{P}_{\nu\lambda'}^0 \right) \right] \\
& (\mu'\nu'|\kappa'\lambda')(\mu\nu|\kappa\lambda) \tag{27}
\end{aligned}$$

$$= \sum_{\mu\nu\kappa\lambda} \sum_{\mu'\nu'\kappa'\lambda'} \text{Re} \left( {}^q\mathbf{P}_{\mu'\mu} {}^q\bar{\mathbf{P}}_{\lambda\nu'} {}^q\mathbf{P}_{\kappa'\kappa} {}^q\bar{\mathbf{P}}_{\nu\lambda'} \right) (\mu'\nu'|\kappa'\lambda')(\mu\nu|\kappa\lambda) \tag{28}$$

$$= \sum_{\mu\nu\kappa\lambda} \text{Re} \left( ({}^q\boldsymbol{\mu}^q \bar{\boldsymbol{\nu}}|\kappa\lambda)(\mu^q \bar{\boldsymbol{\lambda}}|{}^q\boldsymbol{\kappa}\nu) \right) \tag{29}$$

are expressed in terms of two-electron integrals and occupied

$$\begin{aligned}
{}^q\mathbf{P}^{(z)} &= |\omega_z|^{1/4} {}^q\mathbf{C}^o \exp(+\boldsymbol{\varepsilon}^o t_z) ({}^q\mathbf{C}^o)^\dagger \\
&= |\omega_z|^{1/4} \exp(+t_z {}^q\mathbf{P} {}^q\mathbf{F}) {}^q\mathbf{P} \tag{30}
\end{aligned}$$

and virtual quaternion pseudo-density matrices

$$\begin{aligned}
{}^q\bar{\mathbf{P}}^{(z)} &= |\omega_z|^{1/4} {}^q\mathbf{C}^v \exp(-\boldsymbol{\varepsilon}^v t_z) ({}^q\mathbf{C}^v)^\dagger \\
&= |\omega_z|^{1/4} \exp(-t_z {}^q\mathbf{Q} {}^q\mathbf{F}) {}^q\mathbf{Q}. \tag{31}
\end{aligned}$$

Apart from using quaternion rather than scalar Fock and density matrices, the working equations to compute the SO 2C MP2 energy (Eqs. (24) – (27)) and the pseudo-density matrices (Eqs. (30) – (31)) are identical to their NR counterparts. The equations for computing the NR and spin-free (SF) MP2 energy are identical because for the latter only the real part of the quaternion pseudo-densities will be non-zero. The quaternion formalism therefore leads to an easy identification of SO contributions to the MP2 energy: these are due to the imaginary parts of the pseudo-densities.



## D. Schwarz-type integral estimates

In his seminal work on the LT AO-based MP2 Häser introduced integral estimates that are employed for a Schwarz-type screening of transformed integrals.<sup>6</sup> Due to the similarity of the working equations for NR and 2C MP2, the original Schwarz-type screening can be extended easily to discard contributions of AO quadruple to the Coulomb

$$|(\underline{\mu}^{q_1} \bar{\nu}^{q_1} | \kappa \lambda)(\mu \nu | \underline{\kappa}^{q_1} \bar{\lambda}^{q_1})| \leq Z_{\mu\nu}^{q_1 q_1} Q_{\kappa\lambda} Q_{\mu\nu} Z_{\kappa\lambda}^{q_1 q_1} \quad (32)$$

and the exchange contribution

$$|(\underline{\mu}^{q_1} \bar{\nu}^{q_2} | \kappa \lambda)(\mu \bar{\lambda}^{q_2} | \underline{\kappa}^{q_1} \nu)| \leq Z_{\mu\nu}^{q_1 q_2} Q_{\kappa\lambda} Y_{\mu\lambda}^{q_2} X_{\kappa\nu}^{q_1} \quad (33)$$

to the 2C MP2 correlation energy. The (quaternion pseudo-)Schwarz estimates in Eqs. (32) – (33) are given by:

$$(Q_{\mu\nu})^2 = (\mu\nu | \mu\nu), \quad (34)$$

$$(X_{\mu\nu}^{q_1})^2 = \underline{P}_{\mu'\mu}^{q_1} \underline{P}_{\kappa'\mu}^{q_1} (\mu'\nu | \kappa'\nu), \quad (35)$$

$$(Y_{\mu\nu}^{q_1})^2 = \bar{P}_{\nu\nu'}^{q_1} \bar{P}_{\nu\lambda'}^{q_1} (\mu\nu' | \mu\lambda'), \quad (36)$$

$$Z_{\mu\nu}^{q_1 q_2} = \min\left(\sum_{\nu'} X_{\mu\nu'}^{q_1} |\bar{P}_{\nu\nu'}^{q_2}|, \sum_{\mu'} |\underline{P}_{\mu'\mu}^{q_1}| Y_{\mu'\nu}^{q_2}\right). \quad (37)$$

To keep the screening procedure computationally efficient and also retain the rotational invariance of the MP2 energy, the Coulomb (Eq. (32)) and exchange contributions (Eq. (33)) should be screened at the level of shells rather than individual AO basis functions. Thus, for the estimates  $\mathbf{Q}$ ,  ${}^q\mathbf{X}$ ,  ${}^q\mathbf{Y}$ , and  ${}^{q,q}\mathbf{Z}$  the maximum or Frobenius norm computed for all basis functions that are associated with a shell pair are employed for screening.

The Schwarz-type screening of Ref. 6 allows for an  $\mathcal{O}(N^2)$  scaling with the system size  $N$ . However, as it was shown for the NR LT AO-based MP2<sup>8,12</sup> efficient linearly scaling implementations ( $\mathcal{O}(N)$ ) are only in reach if one accounts for the physically correct decay behavior of two charge distributions separated by  $R$ . For the exchange term  $E_K$  fast exponential decay is expected. The familiar  $R^{-6}$  decay of  $E_J$  at large  $R$  is due to the orthogonality of the occupied and virtual orbital space which causes the zeroth-order moments of the multipole expansion of  $1/R$  to vanish.<sup>7,11</sup> This holds for 2C LT AO-based MP2 as well and can be expressed through an analogous orthogonality condition:

$$0 = {}^q \underline{\mathbf{P}}^{(z)} \mathbf{S} {}^q \bar{\mathbf{P}}^{(z)}. \quad (38)$$

Consequently, the efficient distance dependence adaptation of Häser’s integral estimates proposed by Ochsenfeld and his co-workers<sup>12</sup> can be easily adapted to the 2C LT AO-based MP2 implementation to achieve linear scaling eventually.

### III. COMPUTATIONAL DETAILS

The LT AO-based MP2 energy formulation for relativistic 2C Hamiltonians was implemented in a development version of DIRAC. The two-electron integrals were computed with routines provided by the InteRest library.<sup>20</sup> For all HF calculations the molecular mean field X2C Hamiltonian<sup>3</sup> was used. For the preceding 4C HF calculations only the LL and LS type two-electron integrals were calculated.<sup>21</sup> Point-group symmetry was exploited at the HF level for the HX molecules, only. Nuclei were treated as Gaussian charge distributions.<sup>22</sup> For HX (X = F, Cl, Br, I, and At) we froze 2, 10, 18, 36, and 54 core electrons and 2, 6, 26, 40, and 96 anti-core electrons, respectively, and employed the all-electron double-zeta basis set of Dyall.<sup>23</sup> Experimental equilibrium bond distances<sup>24</sup> were used for (HX, X=F,Cl,Br, and I); 0.9168 Å (F), 1.2746 Å (Cl), 1.4144 Å (Br), and 1.6092 Å (I). The HAt bond distance 1.7075 Å was taken from an all-electron calculation of Peterson et al.<sup>25</sup> The geometry of Hg-porphyrin was optimized with symmetry constraints of the  $D_{2h}$  point group by using the Turbomole package<sup>26</sup> and is provided in the supporting information.<sup>18</sup> For the energy and gradient calculation we employed the dispersion-corrected<sup>27</sup> (D3) PBE density functional<sup>28</sup> and the def2-TZVP basis set. For the same calculation, an effective core potential<sup>29</sup> for Hg with 60 core electrons and multipole accelerated density fitting<sup>30</sup> were used for reasons of performance. For the AO-based MP2 calculation of Hg-porphyrin we used the SVP<sup>31</sup> (H,C, and N) and all-electron double-zeta basis<sup>32</sup> sets (Hg) and froze 60 core and 24 anti-core electrons. In case of Ba<sub>2</sub> the all-electron double-zeta basis<sup>32</sup> was employed and the 72 core and 24 anti-core electrons were frozen. The Laplace parameters  $\omega_z$  and  $t_z$  were obtained by the minimax approximation<sup>33</sup> for a fixed number of quadrature points ( $n_z = 18$  for HX,  $n_z = 27$  for Ba<sub>2</sub>, and  $n_z = 1$  for Hg-porphyrin). The errors in MP2 correlation energies for the diatomic molecules caused by the numerical quadrature were always lower than  $10^{-8}$  a. u. as was verified by comparison with a reference (MO-based) implementation.<sup>34</sup> For Hg-porphyrin only the quaternion Schwarz-type estimates were computed, the MP2 correlation energy was not determined.

## IV. RESULTS AND DISCUSSION

### A. Comparison with spinor-based implementations

Compared to the NR formulation, the LT AO-based formulation of MP2 energies for relativistic 2C Hamiltonians requires 16 times more operations for the computation of HTIs. Contraction of HTIs to the MP2 energy has essentially the same scaling as NR for the 2C Coulomb contributions  $e_J^{(z)}$ , and requires a 4 times larger effort for 2C exchange contributions  $e_K^{(z)}$ .

The “SO factor” of 16 in the time-determining transformation step of our purely AO-based formulation is similar to the factor of 16 found for the first half-transformation in the conventional KR spinor-based approach.<sup>34</sup> In both cases this arises from the need to use a quaternion multiplication in the transformation of the second index, which takes  $4 \times 4 = 16$  terms more operations than multiplication of real matrices. In the conventional formalism, also a second half-transformation is required in which the quaternion unit of the second electron becomes active. This leads ultimately to a factor of  $16 \times 4 = 64$  if no symmetry can be used. In practice, one finds that for a spinor-based MP2 implementation the most expensive step is often the initial quarter transformation, which has a theoretical scaling factor of only 4. Furthermore, only part of the spinors are taken as active in correlation calculation, thereby reducing the size of matrices as the index transformation proceeds. Such reductions are particularly effective for heavy elements in which a number of core orbitals (and the associated virtuals with high energies) can be frozen. For larger molecules, in which typically also many lighter elements are present, the reduction in matrix size is smaller and the later steps of the index transformation become important. For such systems the AO-based formalism of the LT should therefore become competitive, also because integral screening can be very effective with the highly localized densities of heavy elements. It was shown for NR LT AO-based MP2 that integral screening leads to low-order<sup>6,7,9</sup> or even linearly scaling implementations<sup>8,12</sup> for medium- and large-sized systems. Thus, screening and the better SO scaling of the LT AO-based approach has the potential for early break-even points with spinor-based approaches.

## B. Effect of the nuclear charge on the energy contributions

Our current implementation does not exploit any sparsity and has a hard  $\mathcal{O}(N^5)$  scaling with the system size  $N$ . To show the potential of screening on the computational work, we analyze the 16 components of  $|({}^q\boldsymbol{\mu}^q\boldsymbol{\nu}|\kappa\lambda)|^2$  from Eqs. (24) – (27) for the halogen hydrides HX ( $X = \text{F, Cl, Br, I, and At}$ ) in Fig. 1. Note that if the nuclei of a linear molecule are located at one of the Cartesian coordinate axes, two of the three imaginary quaternion parts will be identical for symmetry reasons. For HX in Fig. 1 as well as  $\text{Ba}_2$  in Figs. 2 – 3 we chose the z-axis as molecular axis; thus  $q = 2$  and  $q = 3$  are equivalent. The real or SF parts of the quaternion pseudo-densities  ${}^q\mathbf{P}$  and  ${}^q\bar{\mathbf{P}}$  are much larger than the imaginary or SO parts, which allows for the following grouping of HTIs according to the 16 different combinations termed  $(q_1, q_2)$  of  ${}^q\mathbf{P}$  and  ${}^q\bar{\mathbf{P}}$ : (I) only SF densities; (II) one SF and one SO density; (III) two SO densities. As can be seen from Fig. 1, the difference is most distinct for the lightest hydride  $X=\text{F}$  where (I) and (II) differ roughly by a factor of  $10^{-6}$  while (I) and (III) differ by  $10^{-12}$ . For such a light molecule, the energy contributions from HTIs that contain only SO densities are neglected without loss of accuracy if screening is exploited. Since the mixed SF-SO density contributions are small as well, the SF formalism suffices to describe the 2C MP2 energy sufficiently accurate for such a light molecule — the relative deviation to SO 2C MP2 is  $2.8 \times 10^{-6}$  only. The difference between (I) and (II) HTIs and (II) and (III) HTIs decreases by one and two orders of magnitude, respectively, each time we compare with a heavier homologue. For the heaviest halogen hydride HAt the SF-only HTIs and the mixed SF-SO HTIs differ by a factor of  $10^{-2}$  while the former and the SO-only HTIs differ roughly by  $10^{-4}$ . For HAt the relative deviation between SF and 2C MP2 is much larger ( $2.5 \times 10^{-3}$ ) than for  $X=\text{F}$ . Thus, the SF approximation shows only limited accuracy for this small molecule that is dominated by the heavy element. For larger molecules in which one or more heavy atoms are present a complete neglect of SO coupling may likewise lead to significant errors. However, as all HTIs are expressed in the AO basis, it is still possible to obtain considerable savings by only neglecting SO contributions for pseudo density matrix elements of the light elements. Such savings are not possible in conventional MO-based electron correlation treatments.

### C. Distance dependence of the energy contributions and estimates

Besides the nuclear charge, the inter-electronic distance has a substantial effect on screening and its utilization results eventually in a linearly scaling relativistic MP2 implementation.<sup>8,12</sup> First, this distance behavior is investigated by means of the contributions to the interaction energy of Ba<sub>2</sub> in Fig. 2.  $E_J$  shows the typical  $R^{-6}$  decay of the dispersion energy as explained in Sec. II, the 4 contributions to  $E_K$  decay more rapidly than the Coulomb contribution; but the expected exponential scaling is hard to observe as the values result from taking differences between small numbers. Amongst the 4 exchange contribution, the one that includes the SF-only HTIs is clearly the largest while the other 3 contribute only little. It is also clear that the decay of the already small SO contributions  $E_K(q = 1, 2 = 3)$  is at least as fast as the SF  $E_K(0)$  contribution.

Individual elements of the  ${}^q\mathbf{X}$  estimates are shown in Fig. 3 for selected points of the Ba<sub>2</sub> potential curve from Fig. 2. Like in case of the halogen hydrides, the SF part of the  ${}^q\mathbf{X}$  estimates is largest in magnitude, that is, the largest element in  $\mathbf{X}^0$  is always more than a factor of 30 larger than in  $\mathbf{X}^{q_1}$  with  $q_1 = 1, 2 = 3$ . As the inter-atomic distance increases, the largest elements of the two intra-atomic blocks remains almost constant whereas the largest element of the two inter-atomic blocks decreases and is at  $R=50$  a. u. less than  $1.4 \times 10^{-6}$ ,  $6.1 \times 10^{-10}$ , and  $1.4 \times 10^{-7}$  for  $\mathbf{X}^{q_1}$  with  $q_1 = 0, 1, 2 = 3$ , respectively. Thus, individual elements of the SF and SO pseudo-Schwarz estimates, which are used to screen contributions to the 2C MP2 energy, become smaller in magnitude as the inter-atomic distance increases. If contributions to the 2C MP2 energy are screened by means of SF and SO pseudo-Schwarz estimates in Eqs. (35) – (37), reduced- or even linear-scaling implementations can be designed as for NR AO-based MP2.<sup>8,9,12</sup>

Like for HTIs in Fig. 1 and for the contributions to the exchange interaction energy in Fig. 2 the SO part of the estimates  $\mathbf{X}^{q_1}$  with  $q_1 = 1, \dots, 3$  is much smaller than the SF part, too. This will result in a much more efficient computation of the SO, rather than the SF, energy contributions once screening is exploited. Therefore, in practice, it is expected that the inherent “SO factor” of 4 and 16 for the integral contraction and transformation, respectively, is reduced significantly as there are relatively more SO contributions that fall below threshold at larger distances than SF contributions.

## D. Combined effect of the nuclear charge and the inter-electronic distance on screening

To illustrate the joint effects of the nuclear charge from different elements and the inter-electronic distances, we calculated the estimates  ${}^q\mathbf{X}$ ,  ${}^q\mathbf{Y}$ , and some of  ${}^{q,q}\mathbf{Z}$  for Hg-porphyrin as depicted in Fig. 4. Note that as for the linear molecules HX and Ba<sub>2</sub> two of the three imaginary quaternion parts are identical ( $q = 2$  and  $q = 3$ ) because the x- and y-axis of the molecular coordinate system coincide with the  $C_2$  symmetry elements of the  $D_{2h}$  point group.

Since molecules that are mainly composed of a very few heavy metal elements surrounded by organic ligands are highly relevant for synthetic and bio-organic and inorganic chemistry, Hg-porphyrin is an ideal example to investigate. As expected, the shell pairs of light elements in porphyrin make only significant contributions to the SF part of the estimates ( $q = 0$ ). Consequently, the light elements will mainly contribute to SF part of the 2C MP2 energy while Hg dominate the SO part of the 2C MP2 energy.

The largest element in any of the estimates is always one of the Hg-Hg shell pairs, except for  $\mathbf{Y}^0$  where the maximum value is one of the N-N shell pairs. The H-H shell pairs contribute the least to the estimates, especially for the SO type estimates. Furthermore, it can be observed that the closer the light atoms are to Hg the larger are their estimates. For example, consider the C-C blocks, where the 8 C atoms that are neighbors of the N atoms have larger estimates than the remaining 12 C atoms located at the outside and bridges of the porphyrin ring. Since the estimates are employed to screen contributions of shell quadruple to the MP2 correlation energy, we can conclude that the largest contributions, both SF and SO, to the correlation energy originate from the Hg and N atoms and the least from the H atoms. A more detailed analysis and also quantification of the number of screened shell quadruples is beyond the scope of the present work and can be done once the distance-dependent extension of the pseudo-Schwarz estimates is available.

## V. CONCLUSIONS

We presented a formulation that is ready for combining linear-scaling techniques for wave-function methods with relativistic methods that solve the Dirac equation explicitly.

Working equations are given for the LT AO-based MP2 for relativistic 2C Hamiltonians in the KR formalism and compared to their NR counterparts. By an analysis of the norm of HTIs it is shown that for light molecules contributions that arise from taking SO coupling into account can be easily neglected by screening. For molecules with heavy atoms those SO contributions are important and will not be completely neglected when screening is exploited. Furthermore, we have shown that the relativistic 2C Coulomb and exchange contributions to the correlation energy feature the same decay properties with an increasing separation of charge distributions as their NR counterparts. An adaptation of distance-dependent integral estimates developed for NR MP2 to quaternion-based HTIs will therefore result in a linearly scaling 2C MP2 implementation with early break-even points compared to conventional spinor-based implementations. Schwarz-type screening estimates can be adapted easily to the 2C LT AO-based MP2 formalism. Both SF- and SO-type estimates become negligible for large inter-electronic distances. For light elements only the SF-type estimates show sizable contributions, which makes the 2C LT AO-based MP2 formalism attractive for calculation on large metal-organic complexes once a linearly scaling implementation is available.

## VI. ACKNOWLEDGMENTS

Financial support from the German research foundation DFG through grant number HE 7427/1-1 is gratefully acknowledged. MR acknowledges support from the Research Council of Norway through a Centre of Excellence Grant (No. 179568/V30). The authors thank Trond Saue for helpful discussions on the quaternion formulation of the Dirac–Hartree–Fock method.

## REFERENCES

<sup>a</sup>Electronic mail: b.helmichparis@vu.nl

<sup>b</sup>Electronic mail: michal.repisky@uit.no

<sup>c</sup>Electronic mail: l.visscher@vu.nl

<sup>1</sup>K. G. Dyall and K. Fægri, *Introduction to relativistic quantum chemistry* (Oxford University Press, 2007).

- <sup>2</sup>M. Iliáš, H. J. A. Jensen, V. Kellö, B. O. Roos, and M. Urban, *Chem. Phys. Lett.* **408**, 210 (2005); W. Kutzelnigg and W. Liu, *J. Chem. Phys.* **123**, 241102 (2005); *Mol. Phys.* **104**, 2225 (2006); M. Iliáš and T. Saue, *J. Chem. Phys.* **126**, 064102 (2007).
- <sup>3</sup>D. Peng, W. Liu, Y. Xiao, and L. Cheng, *J. Chem. Phys.* **127**, 104106 (2007); W. Liu and D. Peng, **131**, 031104 (2009); J. Sikkema, L. Visscher, T. Saue, and M. Iliáš, **131**, 124116 (2009).
- <sup>4</sup>C. Møller and M. S. Plesset, *Phys. Rev.* **46**, 618 (1934).
- <sup>5</sup>M. Häser and J. Almlöf, *J. Chem. Phys.* **96**, 489 (1992).
- <sup>6</sup>M. Häser, *Theor. Chem. Acc.* **87**, 147 (1993).
- <sup>7</sup>P. Y. Ayala and G. E. Scuseria, *J. Chem. Phys.* **110**, 3660 (1999).
- <sup>8</sup>B. Doser, D. S. Lambrecht, J. Kussmann, and C. Ochsenfeld, *J. Chem. Phys.* **130**, 064107 (2009).
- <sup>9</sup>S. A. Maurer, J. Kussmann, and C. Ochsenfeld, *J. Chem. Phys.* **141**, 051106 (2014); G. Hetzer, M. Schütz, H. Stoll, and H.-J. Werner, **113**, 9443 (2000); Y. Jung, R. C. Lochan, A. D. Dutoi, and M. Head-Gordon, **121**, 9793 (2004); J. Yang, Y. Kurashige, F. R. Manby, and G. K. L. Chan, **134**, 044123 (2011); G. Schmitz, B. Helmich, and C. Hättig, *Mol. Phys.* **111**, 2463 (2013).
- <sup>10</sup>J. Almlöf, *Chem. Phys. Lett.* **181**, 319 (1991).
- <sup>11</sup>D. S. Lambrecht, B. Doser, and C. Ochsenfeld, *J. Chem. Phys.* **123**, 184102 (2005).
- <sup>12</sup>S. A. Maurer, D. S. Lambrecht, J. Kussmann, and C. Ochsenfeld, *J. Chem. Phys.* **138**, 014101 (2013).
- <sup>13</sup>W. Klopper and W. Kutzelnigg, *Chem. Phys. Lett.* **134**, 17 (1987); W. Kutzelnigg and W. Klopper, *J. Chem. Phys.* **94**, 1985 (1991); W. Klopper, F. R. Manby, S. Ten-No, and E. F. Valeev, *International Reviews in Physical Chemistry* **25**, 427 (2006).
- <sup>14</sup>Z. Li, S. Shao, and W. Liu, *J. Chem. Phys.* **136**, 144117 (2012); S. Ten-no and D. Yamaki, **137**, 131101 (2012).
- <sup>15</sup>D. S. Hollman, J. J. Wilke, and H. F. S. III., *J. Chem. Phys.* **138**, 064107 (2013).
- <sup>16</sup>H. A. Kramers, *P. K. Akad. Wet.-Amsterd.* **33**, 959 (1930).
- <sup>17</sup>P. R. Surján, *Chem. Phys. Lett.* **406**, 318 (2005).
- <sup>18</sup>See supplementary material at URL.
- <sup>19</sup>T. Saue, K. Fægri, T. Helgaker, and O. Gropen, *Mol. Phys.* **91**, 937 (1997); T. Saue and H. J. A. Jensen, *J. Chem. Phys.* **111**, 6211 (1999).



- <sup>20</sup>M. Repisky, (2013), InteRest 2.0, An integral program for relativistic quantum chemistry.
- <sup>21</sup>L. Visscher, *Theor. Chem. Acc.* **98**, 68 (1997).
- <sup>22</sup>L. Visscher and K. G. Dyall, *Atomic Data and Nuclear Data Tables* **67**, 207 (1997).
- <sup>23</sup>K. G. Dyall, “All-electron basis sets for the 2p and 3p elements,” unpublished; *Theor. Chem. Acc.* **115**, 441 (2006); *Theor. Chem. Acc.* **131**, 1 (2012).
- <sup>24</sup>K. P. Huber and G. Herzberg, in *NIST Chemistry WebBook, NIST Standard Reference Database Number 69*, edited by P. Linstrom and W. Mallard (National Institute of Standards and Technology, Gaithersburg MD, 20899, 2015) data prepared by J.W. Gallagher and R.D. Johnson, III.
- <sup>25</sup>K. A. Peterson, D. Figgen, E. Goll, H. Stoll, and M. Dolg, *J. Chem. Phys.* **119**, 11113 (2003).
- <sup>26</sup>“TURBOMOLE V7.0 2015, a development of University of Karlsruhe and Forschungszentrum Karlsruhe GmbH, 1989-2007, TURBOMOLE GmbH, since 2007; available from <http://www.turbomole.com>,”.
- <sup>27</sup>S. Grimme, *J. Comput. Chem.* **27**, 1787 (2006); S. Grimme, J. Antony, S. Ehrlich, and H. Krieg, *J. Chem. Phys.* **132**, 154104 (2010).
- <sup>28</sup>J. P. Perdew, M. Ernzerhof, and K. Burke, *J. Chem. Phys.* **105**, 9982 (1996).
- <sup>29</sup>D. Andrae, U. Häußermann, M. Dolg, H. Stoll, and H. Preuss, *Theor. Chim. Acta* **77**, 123 (1990).
- <sup>30</sup>K. Eichkorn, O. Treutler, H. Öhm, M. Häser, and R. Ahlrichs, *Chem. Phys. Lett.* **240**, 283 (1995); **242**, 652 (1995); M. Sierka, A. Hogekamp, and R. Ahlrichs, *J. Chem. Phys.* **118**, 9136 (2003).
- <sup>31</sup>A. Schäfer, H. Horn, and R. Ahlrichs, *J. Chem. Phys.* **97**, 2571 (1992).
- <sup>32</sup>K. G. Dyall, *Theor. Chem. Acc.* **131**, 1 (2012).
- <sup>33</sup>A. Takatsuka, S. Ten-no, and W. Hackbusch, *J. Chem. Phys.* **129**, 044112 (2008); B. Helmich-Paris and L. Visscher, (2016), *J. Comp. Phys.*, accepted for publication, <http://dx.doi.org/10.1016/j.jcp.2016.06.011>.
- <sup>34</sup>J. K. Laerdahl, T. Saue, and K. Fægri, *Theor. Chem. Acc.* **97**, 177 (1997); J. Thyssen, T. Fleig, and H. J. A. Jensen, *J. Chem. Phys.* **129**, 034109 (2008).

## FIGURES

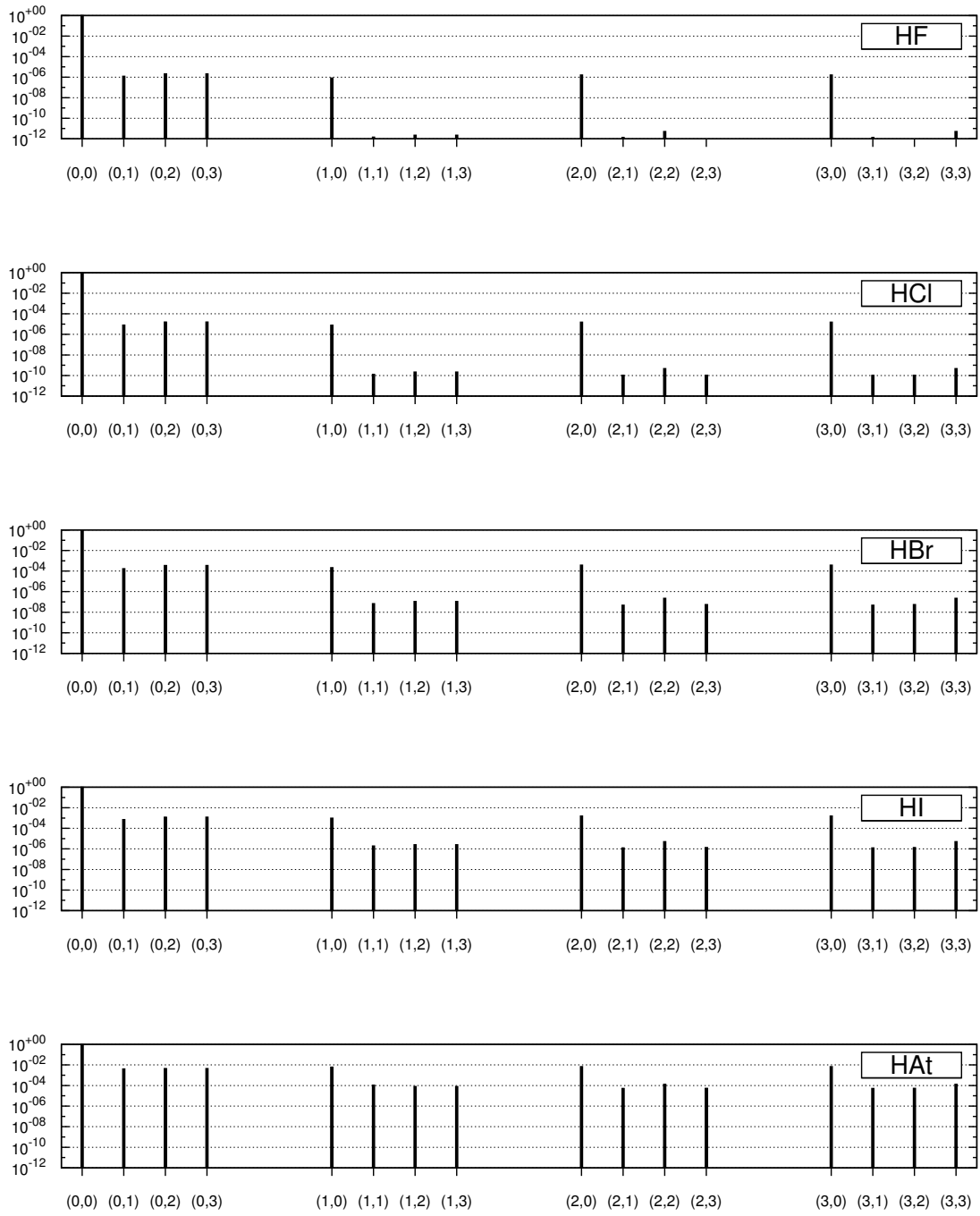


FIG. 1.  $|(\underline{q}\underline{\mu}{}^{\underline{q}}\underline{\nu}|\kappa\lambda)|^2$  of the 16 HTIs summed over all quadrature points and normalized to the largest component (0,0).

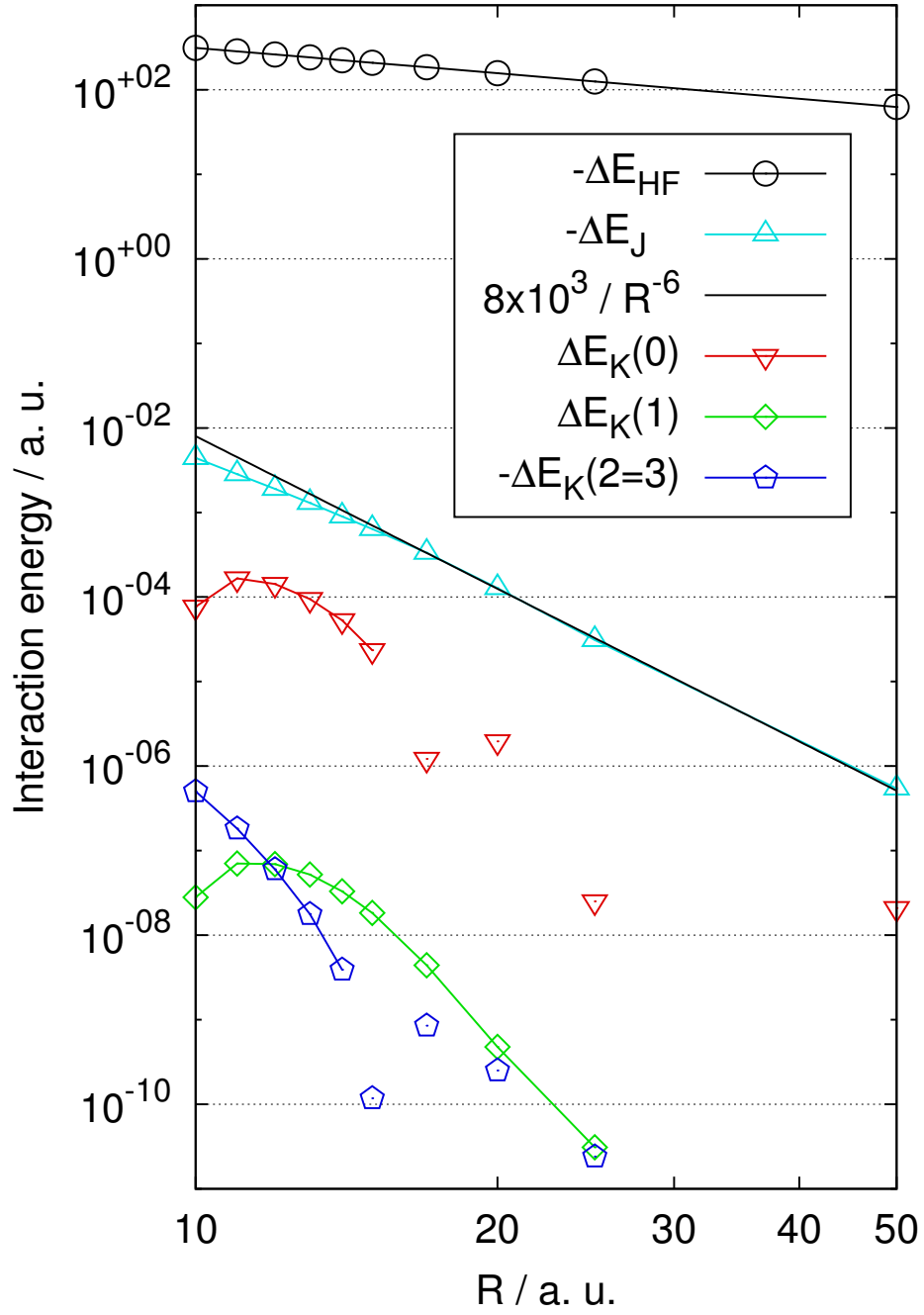


FIG. 2.  $E_J$ ,  $E_K$ , and electronic HF contributions to the SO 2C MP2 interaction energy at different inter-atomic distances  $R$  of the barium dimer.  $\Delta E_K$  points not connected by a line have an opposite sign.

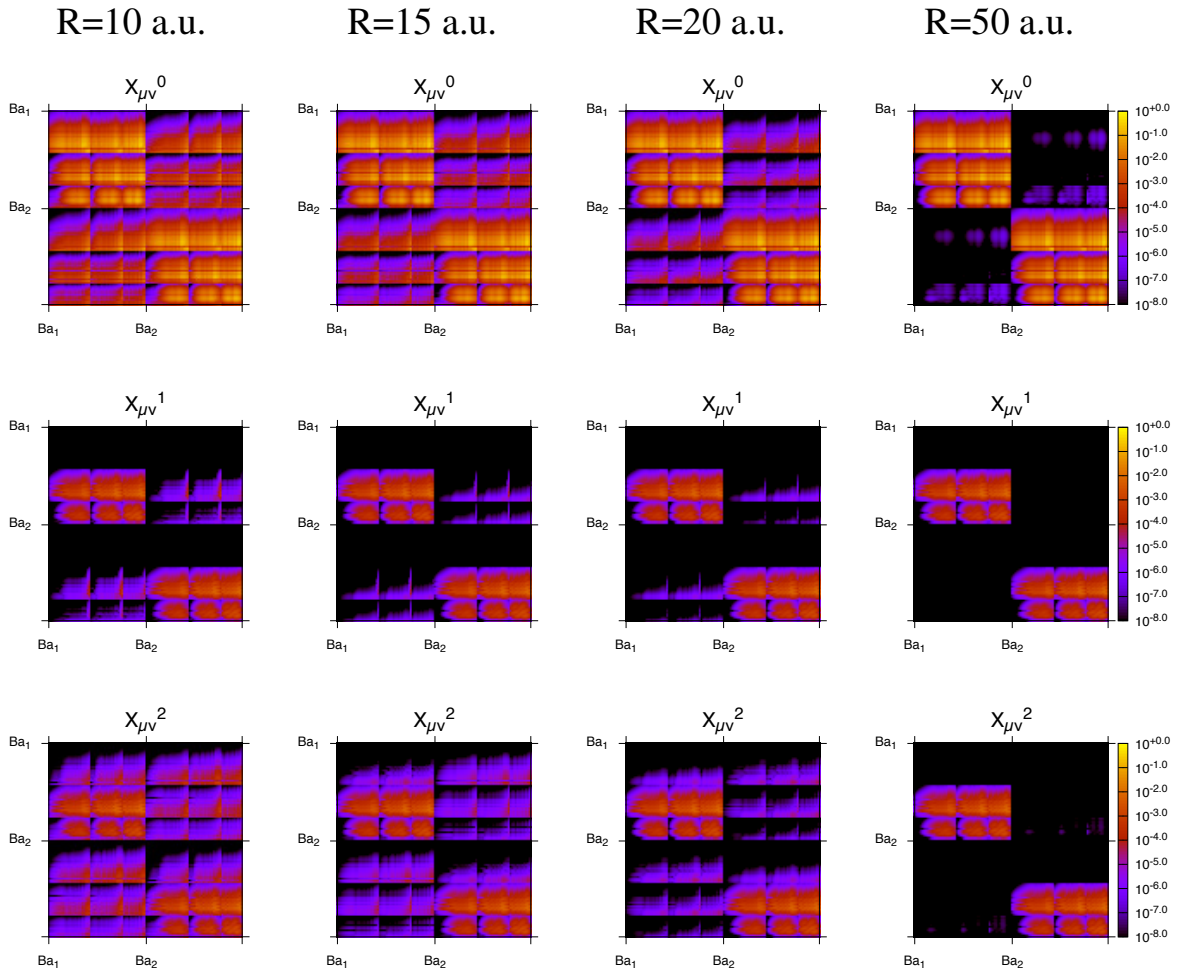


FIG. 3. Individual elements of the estimate  ${}^q\mathbf{X}$  at different inter-atomic distances  $R$  of the barium dimer.

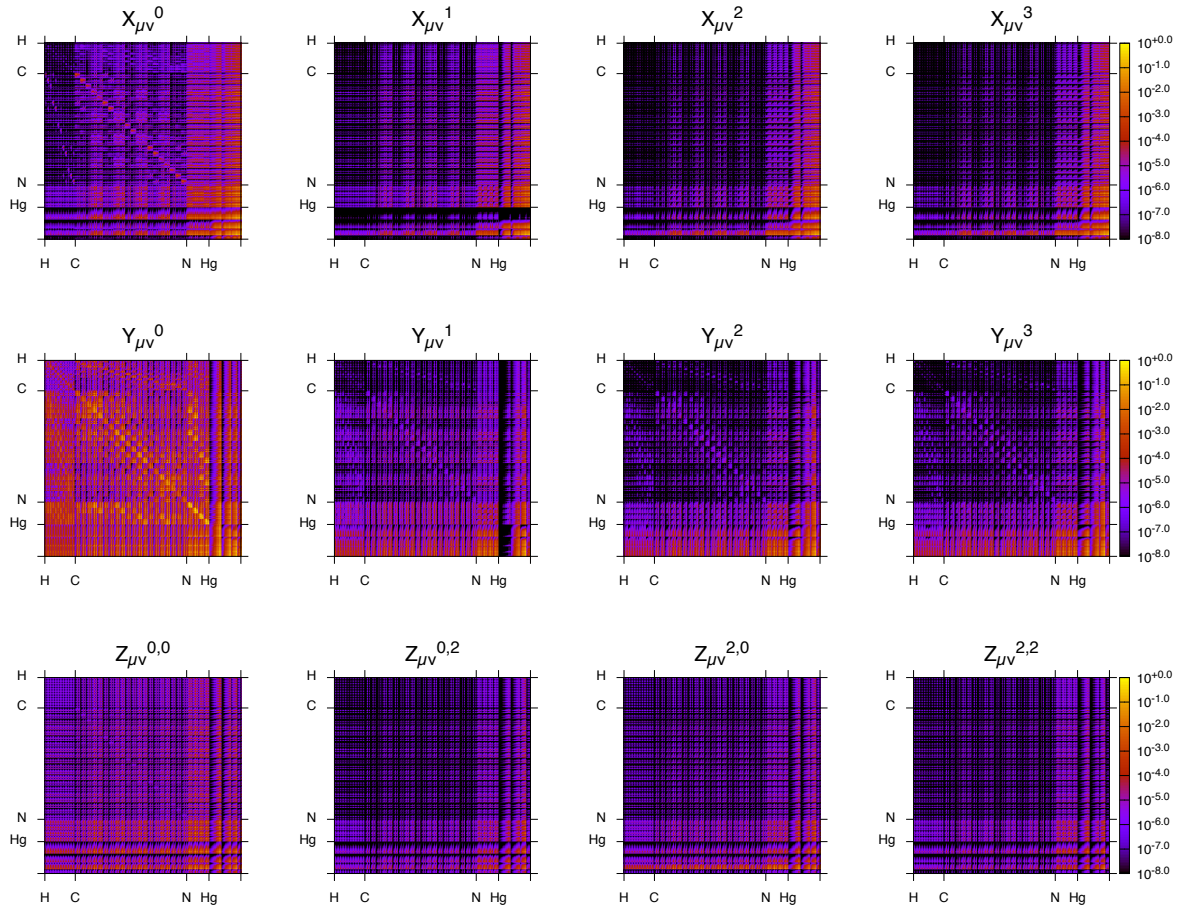


FIG. 4. Individual elements of the estimates  ${}^q\mathbf{X}$  and  ${}^q\mathbf{Y}$  and some selected  ${}^q\mathbf{Z}$  for Hg-porphyrin.